NASA/TM—2011-217135 AAS–11–612

Taylor Series Trajectory Calculations Including Oblateness Effects and Variable Atmospheric Density

James R. Scott
Glenn Research Center, Cleveland, Ohio

August 2011

NASA STI Program . . . in Profile

Since its founding, NASA has been dedicated to the advancement of aeronautics and space science. The NASA Scientific and Technical Information (STI) program plays a key part in helping NASA maintain this important role.

The NASA STI Program operates under the auspices of the Agency Chief Information Officer. It collects, organizes, provides for archiving, and disseminates NASA's STI. The NASA STI program provides access to the NASA Aeronautics and Space Database and its public interface, the NASA Technical Reports Server, thus providing one of the largest collections of aeronautical and space science STI in the world. Results are published in both non-NASA channels and by NASA in the NASA STI Report Series, which includes the following report types:

- TECHNICAL PUBLICATION. Reports of completed research or a major significant phase of research that present the results of NASA programs and include extensive data or theoretical analysis. Includes compilations of significant scientific and technical data and information deemed to be of continuing reference value. NASA counterpart of peer-reviewed formal professional papers but has less stringent limitations on manuscript length and extent of graphic presentations.

- TECHNICAL MEMORANDUM. Scientific and technical findings that are preliminary or of specialized interest, e.g., quick release reports, working papers, and bibliographies that contain minimal annotation. Does not contain extensive analysis.

- CONTRACTOR REPORT. Scientific and technical findings by NASA-sponsored contractors and grantees.

- CONFERENCE PUBLICATION. Collected papers from scientific and technical conferences, symposia, seminars, or other meetings sponsored or cosponsored by NASA.

- SPECIAL PUBLICATION. Scientific, technical, or historical information from NASA programs, projects, and missions, often concerned with subjects having substantial public interest.

- TECHNICAL TRANSLATION. English-language translations of foreign scientific and technical material pertinent to NASA's mission.

Specialized services also include creating custom thesauri, building customized databases, organizing and publishing research results.

For more information about the NASA STI program, see the following:

- Access the NASA STI program home page at *http://www.sti.nasa.gov*

- E-mail your question via the Internet to *help@sti.nasa.gov*

- Fax your question to the NASA STI Help Desk at 443–757–5803

- Telephone the NASA STI Help Desk at 443–757–5802

- Write to:
  NASA Center for AeroSpace Information (CASI)
  7115 Standard Drive
  Hanover, MD 21076–1320

NASA/TM—2011-217135 AAS–11–612

Taylor Series Trajectory Calculations Including Oblateness Effects and Variable Atmospheric Density

James R. Scott
Glenn Research Center, Cleveland, Ohio

Prepared for the
2011 Astrodynamics Specialist Conference
cosponsored by the American Astronautical Society (AAS) and
American Institute of Aeronautics and Astronautics (AIAA)
Girdwood, Alaska, July 31 to August 4, 2011

National Aeronautics and
Space Administration

Glenn Research Center
Cleveland, Ohio 44135

August 2011

This report contains preliminary findings, subject to revision as analysis proceeds.

Level of Review: This material has been technically reviewed by technical management.

Available from

NASA Center for Aerospace Information
7115 Standard Drive
Hanover, MD 21076–1320

National Technical Information Service
5301 Shawnee Road
Alexandria, VA 22312

Available electronically at http://www.sti.nasa.gov

Taylor Series Trajectory Calculations Including Oblateness Effects and Variable Atmospheric Density

James R. Scott
National Aeronautics and Space Administration
Glenn Research Center
Cleveland, Ohio 44135

ABSTRACT

Taylor series integration is implemented in NASA Glenn's Spacecraft N-body Analysis Program, and compared head-to-head with the code's existing 8th- order Runge-Kutta Fehlberg time integration scheme. This paper focuses on trajectory problems that include oblateness and/or variable atmospheric density. Taylor series is shown to be significantly faster and more accurate for oblateness problems up through a 4x4 field, with speedups ranging from a factor of 2 to 13. For problems with variable atmospheric density, speedups average 24 for atmospheric density alone, and average 1.6 to 8.2 when density and oblateness are combined.

INTRODUCTION

We recently demonstrated the significant advantages of Taylor series integration in calculating spacecraft trajectories, i.e., order-of-magnitude speedup and simultaneous improvement in accuracy over a conventional 8th -order Runge-Kutta method.[1] Force models included central body gravitation (including J_2), other body gravitation, thrust, constant atmospheric drag and solar radiation pressure with constant illumination.

In this paper we consider gravitational harmonics beyond J_2 and drag due to variable atmospheric density. We show that Taylor series (TS) offers significant computational advantages in both cases, but also has limitations.

An alternative TS approach for handling oblateness and variable atmospheric density has been presented by Montenbruck.[2] The key differences here are the present implementation applies to spacecraft virtually anywhere in the solar system, can be used interchangeably with another integration method and employs the 1976 Standard Atmosphere[3].

In the next section we summarize the TS methodology for handling oblateness effects and atmospheric density, and discuss its implementation in NASA Glenn's Spacecraft N-body Analysis Program (SNAP)[4]. Following that we present several example problems and discuss numerical results. Head-to-head comparisons are made with SNAP's 8th-order Runge-Kutta Fehlberg (RKF) scheme.[5]

TAYLOR SERIES FORMULATION

The governing equations of spacecraft motion are

$$\begin{aligned} \boldsymbol{x}' &= \boldsymbol{v} \\ \boldsymbol{v}' &= \boldsymbol{a}(x_1, x_2, x_3, x_4, x_5, x_6, x_7, t) \\ x_7' &= -\dot{m}(t) \end{aligned} \tag{1}$$

where $(x_1, x_2, x_3) = \boldsymbol{x}$ is the spacecraft position in Cartesian coordinates relative to an inertial frame centered at the central body, $(x_4, x_5, x_6) = \boldsymbol{v}$ is the velocity, x_7 is the spacecraft mass, $\dot{m}$ is the mass flow rate and $\boldsymbol{a}$ is the acceleration, where

$$\boldsymbol{a} = \boldsymbol{a}_{\mathrm{cb}} + \boldsymbol{a}_{\mathrm{ob}} + \boldsymbol{a}_{\mathrm{th}} + \boldsymbol{a}_{\mathrm{d}} + \boldsymbol{a}_{\mathrm{srp}} + \boldsymbol{a}_{\mathrm{obc}} + \boldsymbol{a}_{\mathrm{obo}} \tag{2}$$

$\boldsymbol{a}$ is the sum of accelerations from the central body point mass, other body point masses, thrust, atmospheric drag, solar radiation pressure, oblateness effects of the central body, and oblateness effects of other bodies.

As described previously[1], the basic approach is to expand each component of the spacecraft state vector $\boldsymbol{X} = (x_1, x_2, x_3, x_4, x_5, x_6, x_7)$ in a local Taylor series which is then used to advance the solution to the next time level. Derivatives are obtained by reformulating Equations (1) into a desired canonical form and then making use of highly efficient differentiation arithmetic. A series expansion is made at each time level *i*,

$$x_n(t) = \sum_{k=0}^{K} X_n(k)\,(t - t_i)^k \ , \tag{3}$$

for n = 1,2, …, N, where N is the number of equations in the reformulated system, and the Taylor coefficients $X_n(k)$ are evaluated through simple recursive formulas.

Oblateness Effects of the Central Body

The gravitational potential due to a non-spherical shaped central body is expressed in the form of a truncated series whose coefficients are obtained from experimental observation. Non-spherical gravity accelerations are readily obtained as the gradient of the potential function. While simple in concept, the mathematical expressions are quite involved and will not be presented here. See Baker[6] (pp. 144-150), Battin[7] (pp. 401-408) or Bate et al[8] (pp. 419-423).

Table 1. Number of Auxiliary Variables per Oblateness Case

n m	0	2	3	4
0	2	33	52	59
1		59	74	90
2		68	90	113
3			99	129
4				138

Due to the complexity of the oblateness equations, the number of series terms employed in the gravitational potential and the need to transform from earth-fixed coordinates to the equator and equinox-of-date framework, the number of auxiliary variables required to handle oblateness effects is significantly higher than that of other acceleration terms. Table 1 summarizes the number of auxiliary variables required up through a 4 x 4 field. Each auxiliary variable corresponds to an additional equation in the differential system. The number of auxiliary variables required for the central body point mass is shown as the n=0, m=0 case, where (n,m) = (degree, order) of the spherical harmonics. Note that the central body point mass requires only two additional equations, whereas J_2 alone requires 33 additional equations. The (4,4) case requires 138 additional equations. Clearly, the increasing number of equations will make the TS method inefficient as oblateness resolution is increased beyond a certain point.

Variable Atmospheric Density

The drag acceleration term $\boldsymbol{a}_{\mathrm{d}}$ is

$$a_{d,1} = c_1 \left[\left(x_4 + c_2 x_2\right)^2 + \left(x_5 - c_2 x_1\right)^2 + x_6^2 \right]^{\frac{1}{2}} \left(x_4 + c_2 x_2\right) \Big/ x_7 \tag{4}$$

$$a_{d,2} = c_1 \left[\left(x_4 + c_2 x_2\right)^2 + \left(x_5 - c_2 x_1\right)^2 + x_6^2 \right]^{\frac{1}{2}} \left(x_5 - c_2 x_1\right) \Big/ x_7 \tag{5}$$

$$a_{d,3} = c_1 \left[\left(x_4 + c_2 x_2\right)^2 + \left(x_5 - c_2 x_1\right)^2 + x_6^2 \right]^{\frac{1}{2}} x_6 \Big/ x_7 \tag{6}$$

where $c_1 = -\frac{1}{2} C_D \cdot A \cdot \rho$, A is the spacecraft area, ρ is the atmospheric density, C_D is the drag coefficient and c_2 = rotation rate of Earth. For spacecraft orbits where ρ varies, it is necessary to calculate the time derivatives of c_1. The first derivative is just

$$\frac{dc_1}{dt} = -\frac{1}{2} C_D A \frac{d\rho}{dt} \tag{7}$$

where

$$\frac{d\rho}{dt} = \frac{\partial \rho}{\partial t} + \frac{\partial \rho}{\partial x_1}\frac{dx_1}{dt} + \frac{\partial \rho}{\partial x_2}\frac{dx_2}{dt} + \frac{\partial \rho}{\partial x_3}\frac{dx_3}{dt} \tag{8}$$

or

$$\frac{d\rho}{dt} = \frac{\partial \rho}{\partial t} + \nabla \rho \cdot \boldsymbol{v} \tag{9}$$

The derivatives of ρ must be obtained from the atmospheric density model. We show how this can be done using the 1976 Standard Atmosphere.

Let the spacecraft altitude h be approximated by

$$h = |\boldsymbol{x}| - r_e \tag{10}$$

where r_e is the radius of the earth. Then

$$\frac{\partial \rho}{\partial x_1} = \frac{\partial \rho}{\partial h}\frac{\partial h}{\partial x_1} = \frac{\partial \rho}{\partial h}\frac{x_1}{|\boldsymbol{x}|} \tag{11}$$

$$\frac{\partial \rho}{\partial x_2} = \frac{\partial \rho}{\partial h}\frac{\partial h}{\partial x_2} = \frac{\partial \rho}{\partial h}\frac{x_2}{|\boldsymbol{x}|} \tag{12}$$

$$\frac{\partial \rho}{\partial x_3} = \frac{\partial \rho}{\partial h}\frac{\partial h}{\partial x_3} = \frac{\partial \rho}{\partial h}\frac{x_3}{|\boldsymbol{x}|} \tag{13}$$

so that

$$\boldsymbol{\nabla}\rho = \frac{\partial \rho}{\partial h}\frac{1}{|\boldsymbol{x}|}\,\boldsymbol{x} \tag{14}$$

Since $\frac{\partial \rho}{\partial t} = 0$ for the 1976 Standard Atmosphere, Equation (9) becomes

$$\frac{d\rho}{dt} = \frac{\partial \rho}{\partial h}\frac{1}{|\boldsymbol{x}|}\,\boldsymbol{x}\cdot\boldsymbol{v} \tag{15}$$

Equation (15) can be evaluated so long as $\frac{\partial \rho}{\partial h}$ can be determined for arbitrary h. Here $\frac{\partial \rho}{\partial h}$ can be approximated using finite differences. For h bracketed by h_i and h_{i+1} in the Standard Atmosphere discretization, $\frac{\rho_{i+1}-\rho_i}{h_{i+1}-h_i}$ approximates $\frac{\partial \rho}{\partial h}$ to at least first order, so $\frac{d\rho}{dt}$ is also known to at least first order.

Equation (15) shows that $\frac{d\rho}{dt}$ is inversely proportional to the magnitude of the position vector. In addition, for a purely circular orbit, $\boldsymbol{x}\cdot\boldsymbol{v} \equiv 0$, so that $\frac{d\rho}{dt}$ is zero. This is consistent with and follows from the fact that density is a function of altitude only in the 1976 Standard Atmosphere. Of course, there are no perfectly circular spacecraft orbits, but in general $\boldsymbol{x}\cdot\boldsymbol{v}$ will be quite small for orbits with small eccentricity. The result is that $\frac{d\rho}{dt}$ will be small and higher time derivatives of density may be negligible in many instances.

APPLICATION TO NEAR EARTH TRAJECTORIES

We consider the following problems. (1) Earth-orbiting satellite with oblateness effects and zero atmospheric drag; (2) Spacecraft spiraling out of earth's gravity well in a low thrust trajectory with oblateness effects and zero atmospheric drag; (3) Earth-orbiting satellite with atmospheric drag and zero oblateness; (4) Earth-orbiting satellite with variable atmospheric drag and oblateness effects; (5) Earth-orbiting satellite with constant atmospheric drag and oblateness effects. For all problems the spacecraft mass is 10,000 kg and the moon and sun are included as other bodies. The drag coefficient is 0.7 and the spacecraft area is 240 square meters. In Problems (1) and (3) - (5), the earth-orbiting satellite is at an inclination of 28.45 degrees with initial altitude 415 km and the trajectory is propagated for 10 days. For Problem 2 the calculation ends when the semimajor axis equals 40,000 km.

All calculations were run on a Dell Poweredge 6950, which has 8 AMD 2.8 GHz processers and 16 GB of RAM. TS calculations used a series with 20 terms for all problems. Both RKF and TS used a local error tolerance defined by $\tau_i = \text{Min}_n\,[\,|x_n|\,\tau + \tau]$ where x_n is the n^{th} variable in the state vector/differential system, and τ denotes the error tolerance parameter.

Problems with Oblateness

We consider Problems 1 and 2, with spherical harmonics having degree and order (n,m) = (2,0), (2,2), (3,3) and (4,4). The tables below show (a) the head-to-head ratio of RKF/TS CPU time, (b) relative L_2 convergence of each method to its τ = 1.e-14 solution and (c) difference between TS and RKF solutions at τ = 1.e-14. Relative L_2 convergence is defined by $|\boldsymbol{x} - \boldsymbol{x_f}| / |\boldsymbol{x_f}|$ where $\boldsymbol{x_f}$ is the final spacecraft position at τ = 1.e-14 and $\boldsymbol{x}$ is the final spacecraft position at larger τ, as listed in the tables. Relative L_2 difference between RKF and TS is defined by $|\boldsymbol{x}_{\mathrm{TS}} - \boldsymbol{x}_{\mathrm{RKF}}| / |\boldsymbol{x}_{\mathrm{RKF}}|$.

Table 2.a CPU ratios, RKF/TS, for Problem 1

(n,m)	(2,0)	(2,2)	(3,3)	(4,4)
τ				
1.e-10	8.61	3.07	2.29	1.61
1.e-11	9.87	3.58	2.57	1.89
1.e-12	12.94	4.12	3.10	2.22
1.e-13	15.14	4.88	3.59	2.68
1.e-14	17.41	5.83	4.31	3.17
Average:	12.80	4.29	3.17	2.31

Table 2.b Relative L_2 convergence levels for Problem 1

	RKF				TS			
(n,m)	(2,0)	(2,2)	(3,3)	(4,4)	(2,0)	(2,2)	(3,3)	(4,4)
τ								
1.e-10	0.42e-06	0.42e-06	0.42e-06	0.42e-06	0.13e-07	0.36e-10	0.13e-09	0.24e-10
1.e-11	0.34e-07	0.34e-07	0.34e-07	0.34e-07	0.56e-08	0.25e-10	0.71e-10	0.54e-10
1.e-12	0.27e-08	0.27e-08	0.26e-08	0.27e-08	0.31e-09	0.79e-10	0.10e-09	0.94e-10
1.e-13	0.22e-09	0.21e-09	0.18e-09	0.20e-09	0.35e-09	0.14e-09	0.47e-10	0.85e-10

Table 2.c Difference between RKF and TS solution for Problem 1

(n,m)	Relative L_2 Difference	Absolute Difference (km)
(2,0)	0.148e-09	0.100e-05
(2,2)	0.322e-10	0.218e-06
(3,3)	0.819e-10	0.554e-06
(4,4)	0.146e-09	0.990e-06

Table 3.a CPU ratios, RKF/TS, for Problem 2

(n,m)	(2,0)	(2,2)	(3,3)	(4,4)
τ				
1.e-10	9.14	3.23	2.36	1.74
1.e-11	10.60	3.74	2.76	2.03
1.e-12	12.55	4.45	3.27	2.39
1.e-13	15.32	5.23	3.86	2.83
1.e-14	17.72	6.16	4.53	3.34
Average:	13.07	4.56	3.35	2.47

Table 3.b Relative L_2 convergence levels for Problem 2

	RKF				TS			
(n,m)	(2,0)	(2,2)	(3,3)	(4,4)	(2,0)	(2,2)	(3,3)	(4,4)
τ								
1.e-10	0.13e-04	0.13e-04	0.13e-04	0.13e-04	0.32e-05	0.21e-07	0.15e-08	0.10e-08
1.e-11	0.11e-05	0.11e-05	0.11e-05	0.11e-05	0.87e-07	0.18e-08	0.32e-09	0.86e-09
1.e-12	0.83e-07	0.83e-07	0.83e-07	0.83e-07	0.30e-07	0.77e-09	0.25e-09	0.12e-08
1.e-13	0.59e-08	0.58e-08	0.63e-08	0.61e-08	0.58e-08	0.13e-09	0.85e-09	0.16e-09

Table 3.c Difference between RKF and TS solution for Problem 2

(n,m)	Relative L_2 Difference	Absolute Difference (km)
(2,0)	0.526e-07	0.210e-02
(2,2)	0.662e-07	0.265e-02
(3,3)	0.753e-07	0.301e-02
(4,4)	0.769e-07	0.308e-02

Average TS speedups range from 2.31 to 12.8 for Problem 1, and from 2.47 to 13.07 for Problem 2. Tables 2.b and 3.b show that TS is more converged than RKF in all but one case. CPU times versus convergence levels are plotted in Figures 1 and 2.

The small differences in RKF and TS solutions shown in Tables 2.c and 3.c are due to the fact that TS calculates the motion of the sun and moon, whereas RKF obtains their motion from ephemeris files. The differences are bigger in Problem 2 because the trajectory is propagated over 112 days versus 10 days for Problem 1.

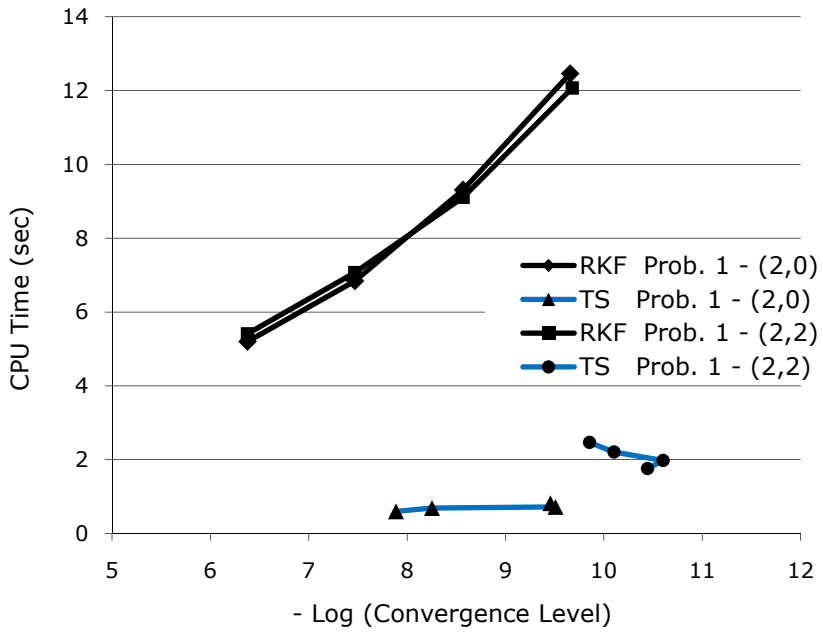

Figure 1.a CPU time vs. valid digits for Problem 1, (n,m) = (2,0), (2,2)

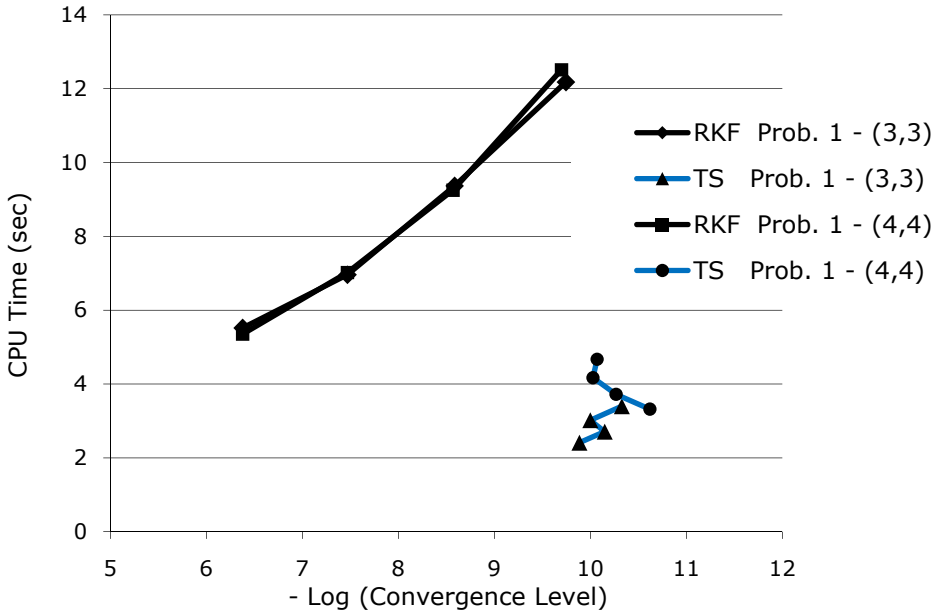

Figure 1.b CPU time vs. valid digits for Problem 1, (n,m) = (3,3), (4,4)

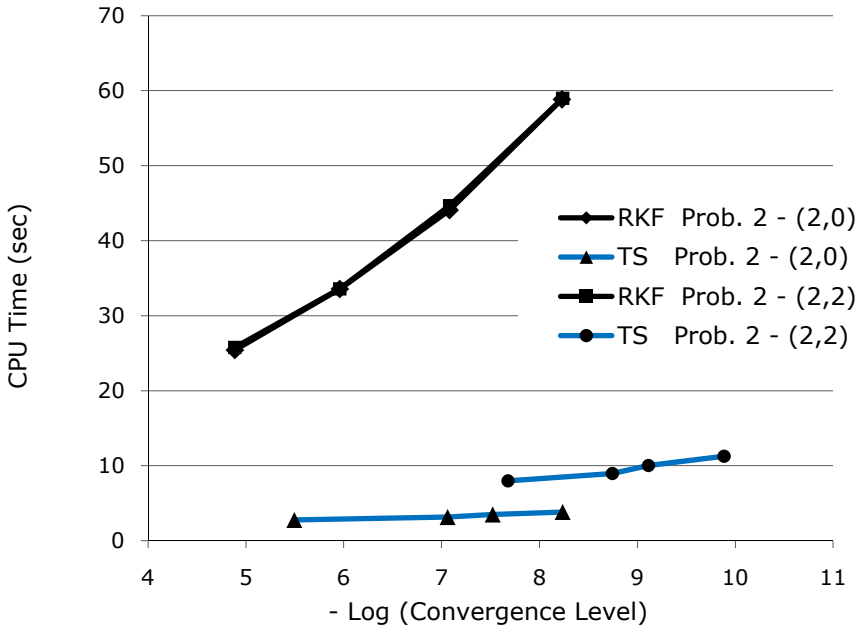

Figure 2.a CPU time vs. valid digits for Problem 2, (n,m) = (2,0), (2,2)

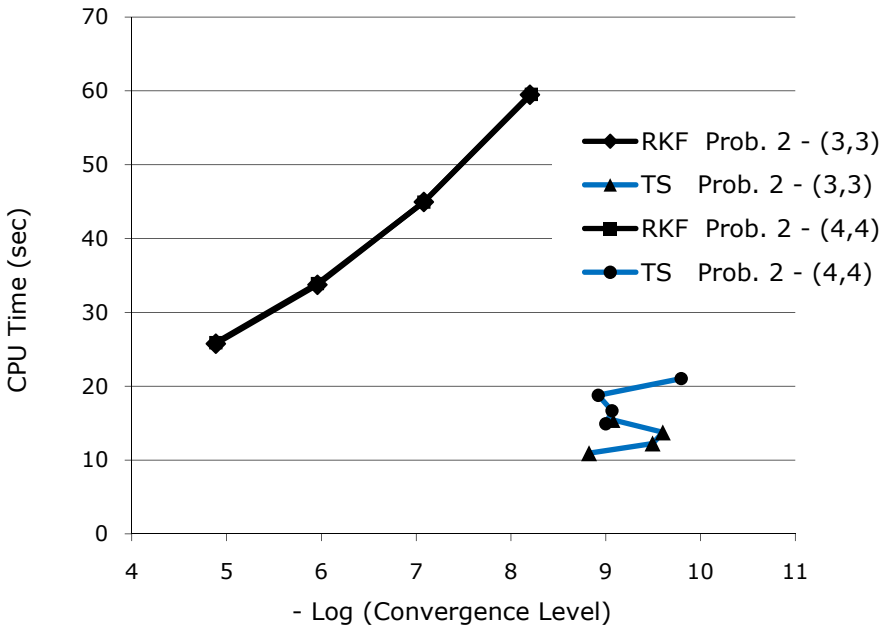

Figure 2.b CPU time vs. valid digits for Problem 2, (n,m) = (3,3), (4,4)

Problems with Atmospheric Drag

Table 4. Effect of Time Derivative Density Term on Results

	Difference in RKF and TS spacecraft position (km)	
	Without Variable Density Model	With Variable Density Model
τ		
1.e-10	0.0306	0.00058
1.e-11	0.0292	0.00189
1.e-12	0.0256	0.00153
1.e-13	0.0230	0.00148
1.e-14	0.0205	0.00124

We present results for an earth-orbiting satellite with atmospheric drag but no oblateness (Problem 3). We first consider the effect of the time derivative density term $\frac{dc_1}{dt}$. Table 4 shows the difference in RKF and TS spacecraft positions after the satellite trajectory has been propagated for 10 days, where the TS trajectory is propagated with and without $\frac{dc_1}{dt}$. The results clearly show the improvement in accuracy due to inclusion of the time derivative density term.

Table 5 summarizes RKF and TS performance on Problem 3. Constant density results are included for comparison. The speedups are quite large here due to the fact that TS can handle the drag equations with only four auxiliary variables. Figure 3 plots the CPU times versus convergence levels.

Table 5.a CPU ratios, RKF/TS, for Problem 3

τ	Constant Density	Variable Density
1.e-10	23.38	17.39
1.e-11	28.82	19.85
1.e-12	34.84	23.30
1.e-13	40.77	28.22
1.e-14	47.90	33.41
Average:	35.14	24.43

Table 5.b Relative L_2 convergence levels for Problem 3

	RKF		TS	
τ	Constant Density	Variable Density	Constant Density	Variable Density
1.e-10	0.43e-06	0.44e-06	0.68e-08	0.17e-06
1.e-11	0.35e-07	0.35e-07	0.10e-09	0.13e-06
1.e-12	0.27e-08	0.28e-08	0.37e-09	0.46e-07
1.e-13	0.20e-09	0.20e-09	0.57e-10	0.36e-07

Table 5.c Difference between RKF and TS solution for Problem 3

Constant Density		Variable Density	
Relative L_2 Difference	Absolute Difference (km)	Relative L_2 Difference	Absolute Difference (km)
0.117e-10	0.794e-07	0.182e-06	0.124e-02

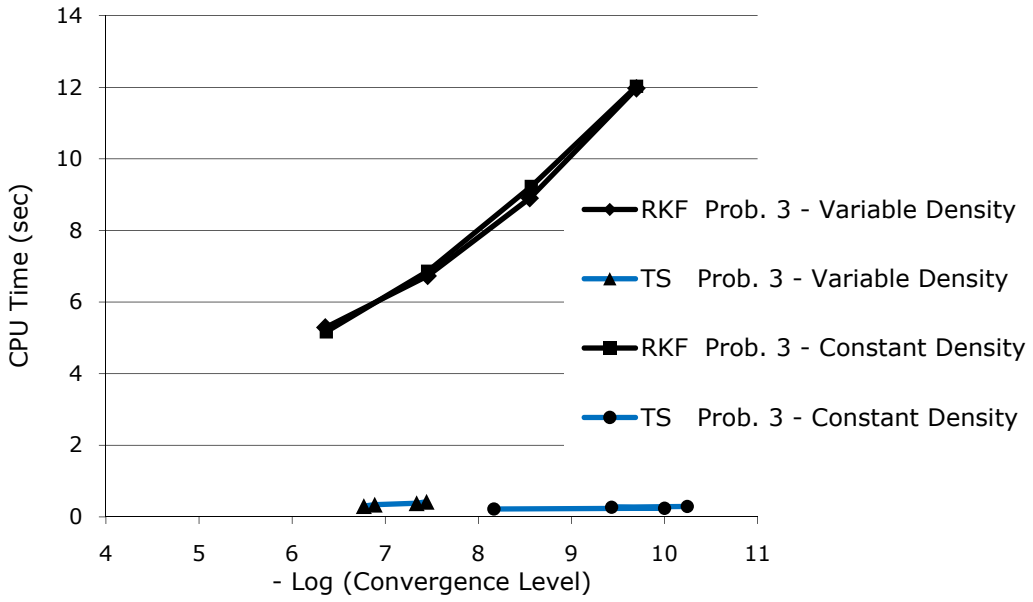

Figure 3. CPU time vs. valid digits for Problem 3

Problems with Atmospheric Drag and Oblateness

We consider Problems 4 and 5. RKF and TS performance are summarized below and results are plotted in the figures which follow. Average TS speedups range from 1.6 to 8.2 for Problem 4 and from 2.2 to 11.9 for Problem 5. The largest absolute difference between RKF and TS shown in Table 6.c is 81.8 meters. It is also worth noting that RKF and TS both predict a reduction in the orbit semimajor axis of 2.709 km (for the (4,4) case). This compares with the drag-only case (Problem 3) in which both methods predict a reduction in semimajor axis of 1.906 km. Atmospheric drag combined with earth's oblateness thus leads to a significantly greater loss in spacecraft altitude.

Table 6.a CPU ratios, RKF/TS, for Problem 4

(n,m)	(2,0)	(2,2)	(3,3)	(4,4)
τ				
1.e-10	5.89	2.12	1.55	1.13
1.e-11	6.84	2.47	1.81	1.32
1.e-12	7.96	2.88	2.09	1.53
1.e-13	9.19	3.41	2.45	1.84
1.e-14	11.03	3.98	2.88	2.17
Average:	8.18	2.97	2.16	1.60

Table 6.b Relative L_2 convergence levels for Problem 4

	RKF				TS			
(n,m)	(2,0)	(2,2)	(3,3)	(4,4)	(2,0)	(2,2)	(3,3)	(4,4)
τ								
1.e-10	0.42e-06	0.43e-06	0.43e-06	0.43e-06	0.40e-05	0.20e-04	0.14e-04	0.12e-04
1.e-11	0.35e-07	0.36e-07	0.34e-07	0.37e-07	0.12e-05	0.13e-04	0.86e-05	0.73e-05
1.e-12	0.10e-08	0.36e-08	0.28e-08	0.48e-08	0.94e-05	0.92e-05	0.44e-05	0.44e-05
1.e-13	0.92e-09	0.22e-08	0.73e-09	0.48e-09	0.77e-05	0.36e-05	0.20e-05	0.19e-05

Table 6.c Difference between RKF and TS solution for Problem 4

(n,m)	Relative L_2 Difference	Absolute Difference (km)
(2,0)	0.881e-06	0.597e-02
(2,2)	0.121e-04	0.818e-01
(3,3)	0.856e-05	0.579e-01
(4,4)	0.732e-05	0.495e-01

Table 7.a CPU ratios, RKF/TS, for Problem 5

(n,m)	(2,0)	(2,2)	(3,3)	(4,4)
τ				
1.e-10	8.14	2.98	2.12	1.62
1.e-11	9.44	3.43	2.52	1.84
1.e-12	11.87	4.03	2.92	2.18
1.e-13	13.70	4.72	3.44	2.53
1.e-14	16.42	5.71	4.07	3.05
Average:	11.91	4.17	3.02	2.24

Table 7.b Relative L_2 convergence levels for Problem 5

	RKF				TS			
(n,m)	(2,0)	(2,2)	(3,3)	(4,4)	(2,0)	(2,2)	(3,3)	(4,4)
τ								
1.e-10	0.42e-06	0.42e-06	0.42e-06	0.42e-06	0.29e-07	0.13e-09	0.69e-10	0.88e-10
1.e-11	0.34e-07	0.34e-07	0.34e-07	0.34e-07	0.39e-08	0.45e-10	0.67e-10	0.39e-10
1.e-12	0.27e-08	0.27e-08	0.27e-08	0.26e-08	0.34e-09	0.48e-10	0.39e-10	0.75e-10
1.e-13	0.20e-09	0.15e-09	0.21e-09	0.21e-09	0.51e-10	0.14e-09	0.71e-10	0.45e-10

Table 7.c Difference between RKF and TS solution for Problem 5

(n,m)	Relative L_2 Difference	Absolute Difference (km)
(2,0)	0.843e-10	0.570e-06
(2,2)	0.282e-10	0.191e-06
(3,3)	0.700e-10	0.474e-06
(4,4)	0.563e-10	0.381e-06

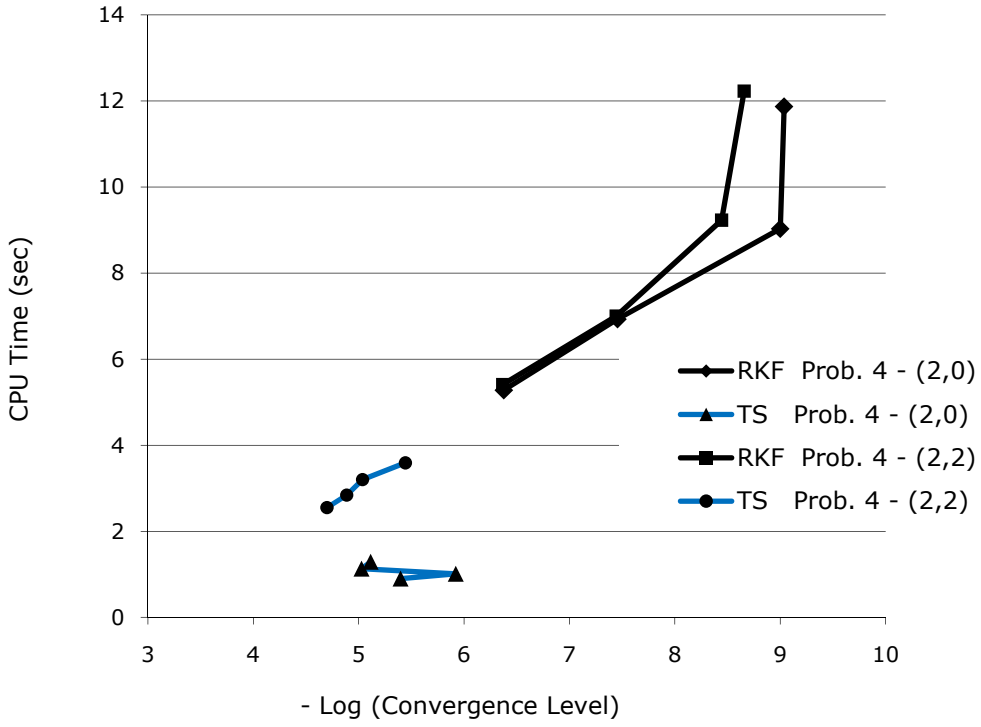

Figure 4.a CPU time vs. valid digits for Problem 4, (n,m) = (2,0), (2,2)

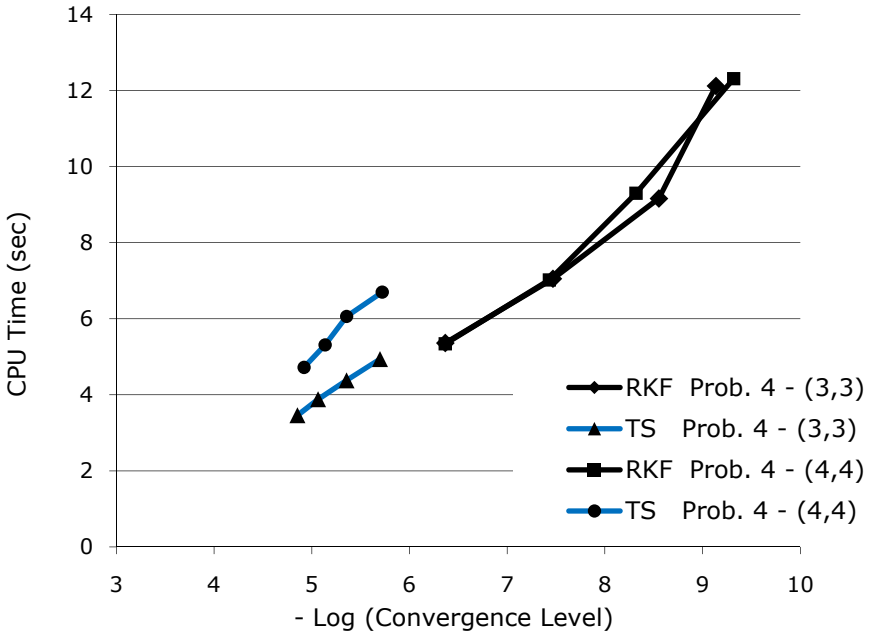

Figure 4.b CPU time vs. valid digits for Problem 4, (n,m) = (3,3), (4,4)

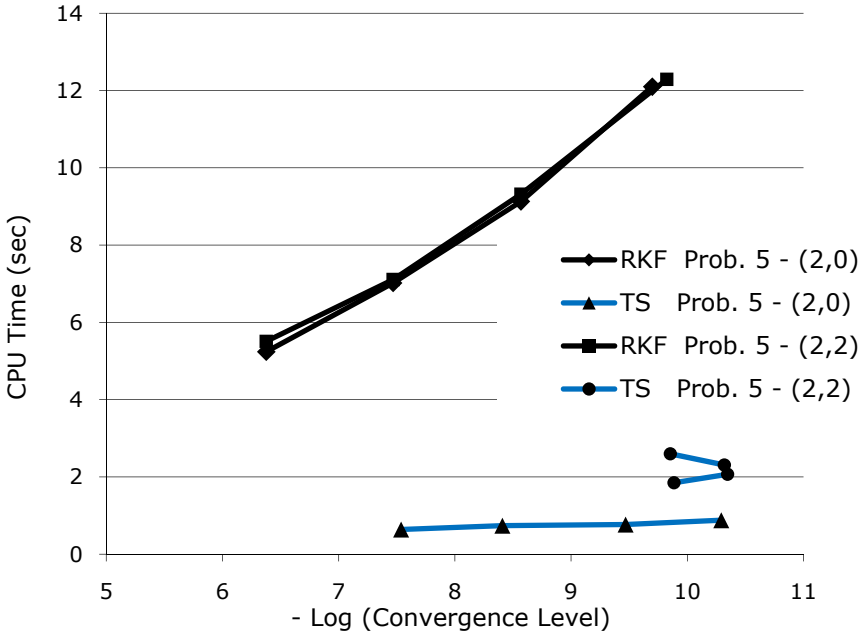

Figure 5.a CPU time vs. valid digits for Problem 5, (n,m) = (2,0), (2,2)

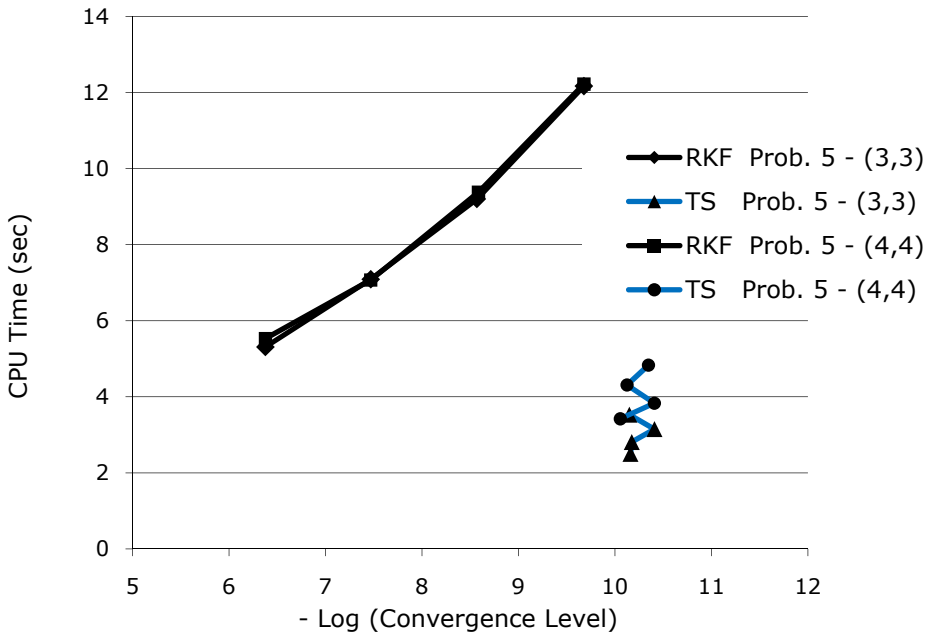

Figure 5.b CPU time vs. valid digits for Problem 5, (n,m) = (3,3), (4,4)

CONCLUSION

Taylor series integration is implemented in a high fidelity trajectory propagation code and applied to near earth trajectory problems. Head-to-head comparisons are made with 8th-order Runge-Kutta Fehlberg integration. Results show that TS is faster by a factor of 2-13 for oblateness problems up through a 4x4 field, while simultaneously improving accuracy. For problems including both oblateness and variable atmospheric density, TS is faster by a factor of 1.6 to 8.2. We conclude that TS is a highly competitive integration method for realistic trajectory problems involving oblateness and atmospheric density.

REFERENCES

[1] Scott, J.R. and Martini, M.C., "High Speed Solution of Spacecraft Trajectory Problems Using Taylor Series Integration," *Journal of Spacecraft and Rockets*, Vol. 47, No. 1, Jan.-Feb. 2010, pp. 199-202; also presented as paper no. AIAA 2008-6957 at the AIAA/AAS Astrodynamics Specialist Conference and Exhibit, 18-21 Aug. 2008, Honolulu, Hawaii.

[2]Montenbruck, O., "Numerical Integration of Orbital Motion Using Taylor Series," *American Astronautical Society/AIAA Spaceflight Mechanics Meeting*, American Astronautical Society Paper 92-195, Feb. 1992.

[3] "1976 U.S. Standard Atmosphere", NOAA, NASA, USAF, U.S. Government Print Office, Washington, D.C., October 1976.

[4]Martini, M.C., "S.N.A.P. 2.3 User's Manual, Spacecraft N-Body Analysis Program," Analex Corporation, Glenn Research Center, Cleveland, OH, 2005.

[5]Fehlberg, E., "Classical Fifth-, Sixth-, Seventh-, and Eighth-Order Runge-Kutta Formulas with Stepsize Control," NASA TR R-287, Oct. 1968.

[6]Baker, R., *Astrodynamics: Applications and Advanced Topics,* Academic Press, New York and London, 1976.

[7]Battin, R., *An Introduction to the Mathematics and Methods of Astrodynamics, Revised Edition*, AIAA Education Series, J. Przemieniecki Editor-in-Chief, American Institute of Aeronautics and Astronautics, Inc., Reston, VA, 1999.

[8]Bate, R., Mueller, D., and White, J., *Fundamentals of Astrodynamics*, Dover Publications, Inc., New York, 1971.

REPORT DOCUMENTATION PAGE			Form Approved OMB No. 0704-0188

1. REPORT DATE *(DD-MM-YYYY)*	2. REPORT TYPE	3. DATES COVERED *(From - To)*
01-08-2011	Technical Memorandum	

4. TITLE AND SUBTITLE
Taylor Series Trajectory Calculations Including Oblateness Effects and Variable Atmospheric Density

5a. CONTRACT NUMBER

5b. GRANT NUMBER

5c. PROGRAM ELEMENT NUMBER

6. AUTHOR(S)
Scott, James, R.

5d. PROJECT NUMBER

5e. TASK NUMBER

5f. WORK UNIT NUMBER
WBS 136905.02.09.03.04

7. PERFORMING ORGANIZATION NAME(S) AND ADDRESS(ES)
National Aeronautics and Space Administration
John H. Glenn Research Center at Lewis Field
Cleveland, Ohio 44135-3191

8. PERFORMING ORGANIZATION REPORT NUMBER
E-17871

9. SPONSORING/MONITORING AGENCY NAME(S) AND ADDRESS(ES)
National Aeronautics and Space Administration
Washington, DC 20546-0001

10. SPONSORING/MONITOR'S ACRONYM(S)
NASA

11. SPONSORING/MONITORING REPORT NUMBER
NASA/TM-2011-217135

12. DISTRIBUTION/AVAILABILITY STATEMENT
Unclassified-Unlimited
Subject Categories: 13 and 64
Available electronically at http://www.sti.nasa.gov
This publication is available from the NASA Center for AeroSpace Information, 443-757-5802

13. SUPPLEMENTARY NOTES

14. ABSTRACT
Taylor series integration is implemented in NASA Glenn's Spacecraft N-body Analysis Program, and compared head-to-head with the code's existing 8th- order Runge-Kutta Fehlberg time integration scheme. This paper focuses on trajectory problems that include oblateness and/or variable atmospheric density. Taylor series is shown to be significantly faster and more accurate for oblateness problems up through a 4 by 4 field, with speedups ranging from a factor of 2 to 13. For problems with variable atmospheric density, speedups average 24 for atmospheric density alone, and average 1.6 to 8.2 when density and oblateness are combined.

15. SUBJECT TERMS
Taylor series; Spacecraft trajectories; Runge-Kutta method; Trajectory analysis; Spacecraft N-body Analysis Program (SNAP); Numberical integration; High order

16. SECURITY CLASSIFICATION OF:			17. LIMITATION OF ABSTRACT	18. NUMBER OF PAGES	19a. NAME OF RESPONSIBLE PERSON
a. REPORT	b. ABSTRACT	c. THIS PAGE			19b. TELEPHONE NUMBER *(include area code)*
U	U	U	UU	20	443-757-5802

STI Help Desk (email:help@sti.nasa.gov)